FeP Nanocatalyst with Preferential [010] Orientation Boosts Hydrogen Evolution Reaction in Polymer-Electrolyte Membrane Electrolyzer

Foteini M. Sapountzi,[a] Elena D. Orlova,[b] Juliana P. S. Sousa,[b] Laura M. Salonen,[b] Oleg I. Lebedev,[c] Georgios Zafeiropoulos,[d] Mihalis N. Tsampas,[d] Hans (J.W.) Niemantsverdriet,[a] Yury V. Kolen'ko,[b]*

[a]Syncat@DIFFER, Syngaschem BV, PO Box 6336, 5600 HH Eindhoven, The Netherlands

[b]International Iberian Nanotechnology Laboratory (INL), Avenida Mestre José Veiga, 4715-330 Braga, Portugal

[c]Laboratoire CRISMAT, UMR 6508, CNRS-Ensicaen, Caen 14050, France

[d]Dutch Institute for Fundamental Energy Research (DIFFER), De Zaale 20, 5612AJ Eindhoven, The Netherlands

CORRESPONDING AUTHOR

*yury.kolenko@inl.int (Yu. V. Kolen'ko), nanochemgroup.org

ABSTRACT

The development of non-precious metal electrocatalysts for polymer-electrolyte membrane (PEM) water electrolysis is a milestone for the technology, which currently relies on rare and expensive platinum-group metals. Half-cell measurements have shown iron phosphide materials to be promising alternative hydrogen evolution electrocatalysts, but their realistic performance in flow-through devices remains unexplored. To fill this gap, we report herein the activity and durability of FeP nanocatalyst under application-relevant conditions. Our facile synthesis route proceeds via impregnation of an iron complex on conductive carbon support followed by phosphorization, giving rise to highly crystalline nanoparticles with predominantly exposed [010] facets, which accounts for the high electrocatalytic activity. The performance of FeP gas diffusion electrodes towards hydrogen evolution was examined under application-relevant conditions in a single cell PEM water electrolysis at 22 °C. The FeP cathode exhibited a current density of 0.2 A cm^{-2} at 2.06 V, corresponding to a difference of merely 0.07 W cm^{-2} in power input as compared to state-of-the-art Pt cathode, while outperforming other non-precious cathodes operated at similar temperature. Quantitative product analysis of our PEM device excluded the presence of side reactions and provided strong experimental evidence that our cell operates with 84–100% Faradaic efficiencies and with 4.1 kWh Nm^{-3} energy consumption. The FeP cathodes exhibited stable performance of over 100 h at constant operation, while their suitability with the intermittency of renewable sources was demonstrated upon 36 h operation at variable power inputs. Overall, the performance as well as our preliminary cost analysis reveal the high potential of FeP for practical applications.

GRAPHICAL ABSTRACT

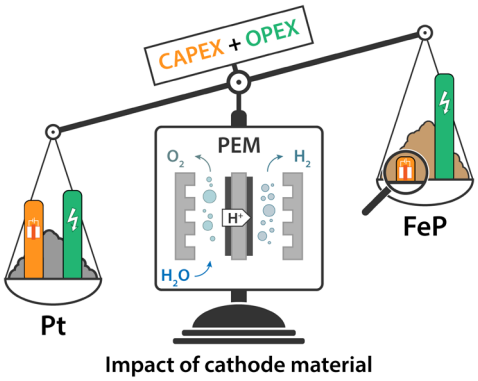

1. Introduction

Hydrogen, H_2, plays an important role in future clean energy technologies as a vector for energy storage.[1] In addition to its high specific energy, it is an environmentally friendly zero-emission fuel with only water as combustion product. Therefore, it is important to develop clean, scalable, and affordable methods for hydrogen production.[2] Water electrolysis, $2H_2O \rightleftharpoons O_2 + 2H_2$, is one of the most attractive ways of producing pure hydrogen. It consists of two half reactions, the hydrogen evolution reaction (HER) and the oxygen evolution reaction (OER), which, under acidic conditions, traditionally rely on platinum- and iridium-based catalysts, respectively.[3] Platinum-group metals are, however, expensive and critical raw materials,[4] and hence their replacement by inexpensive, efficient catalysts featuring earth-abundant elements is of utmost importance, and has led to extensive research effort in the area.[5–8]

Electrocatalysts based on 3d transition metals (TMs), such as Fe, Co, and Ni, have attracted significant attention due to their favorable Gibb's free energy change values, ΔG, for hydrogen activation.[1,9] Although metallic TMs feature rather low electrocatalytic activity, stability, and durability, significant improvements can be made by the introduction of non-metal elements, such as S, N, B, C, and P. Specifically, transition metal phosphides (TMPs) have emerged as highly

active earth-abundant catalysts towards HER.[2,4,10] In this regard, we have developed facile synthesis routes for self-supported Ni–P and Al–Ni–P electrocatalysts, which outperformed most state-of-the-art HER electrocatalysts based on earth-abundant materials.[11–13] In order to reduce the high TMP mass loading of these electrodes to the order of 1 mg cm^{-2} while maintaining the high electrocatalytic activity, we developed a Fe–Ni–P catalyst supported on C-paper based on gas transport phosphorization of a Permalloy precursor.[14] The resulting $Fe_{0.2}Ni_{0.8}P_2$/C paper catalyst showed excellent electrocatalytic performance towards HER both in acidic and alkaline media. On the other hand, we recently prepared cubic NiP_2 cathodes by incorporating nanoparticles into porous gas diffusion layers, which gave highly promising results in HER under industry-relevant conditions.[15] After optimizing the electrode design in terms of NiP_2 and binder loading, the NiP_2 cathodes were introduced in membrane electrode assemblies (MEAs) and tested in a polymer-electrolyte membrane (PEM) electrolysis single cell, requiring merely 13% higher overpotentials than the state-of-the-art Pt/Nafion/$IrRuO_x$ assembly.

Recently, FeP has gained considerable attention in the literature,[16–26] since it has shown high catalytic activity towards HER, even outperforming NiP_2 in half-cell measurements.[27] However, its performance under realistic conditions in flow-through PEM water electrolysis remains unexplored. We report herein a novel, facile, and scalable synthesis of nanocrystalline FeP catalyst, FeP/C, supported on conductive carbon to enhance the electronic conductivity and dispersion of the TMP component.[28,29] To form a 3D electrode architecture, the FeP/C catalyst was subsequently introduced onto C-cloth. The resulting gas diffusion electrodes were integrated into MEAs with Nafion 115 and a commercial $IrRuO_x$ anode. A comparison with the few existing examples of non-precious metal cathodes in application-relevant full-cell PEM water electrolysis reveals that our FeP cathode outperforms others tested at similar temperatures. In addition, quantitative product

analysis via mass spectrometry provided strong experimental evidence that up to 100% Faradaic efficiencies can be reached with FeP based PEM water electrolyzers. Finally, in view of practical applications, the durability of the FeP cathodes was assessed both during 100 h of constant potentiostatic operation as well as under variable power input during 36 h, proving the excellent compatibility of our material with the intermittency of renewable energy sources.

2. Materials and Methods

2.1. Synthesis of carbon-supported FeP nanoparticle catalyst

A solution of $Fe(acac)_3$ in CH_2Cl_2, prepared taking into account the solubility of the iron complex in CH_2Cl_2 of ca. 20 g in 100 mL, was applied to a VULCAN XCmax conductive carbon support (CABOT) by incipient wetness impregnation, which was performed in consecutive cycles to achieve a loading of 20 wt% of Fe phase. The pore volume was estimated by Barrett–Joyner–Halenda (BJH) method to be 1.478 $cm^3\ g^{-1}$. After each impregnation cycle, the material was dried at 100 °C for 10 min. The resulting sample was subjected to one-step gas transport phosphorization under inert atmosphere of argon. Specifically, 0.3 g of P red was loaded into an alumina combustion boat and placed at the beginning of the hot zone of a programmable tube furnace (Lenton), equipped with a quartz tube (inner diameter = 25 mm), and 0.2 g of the sample was placed in the hot zone of the furnace next to the P red at a distance of ca. 3 cm. The phosphorization was conducted under continuous Ar gas flow of 50 mL min^{-1}. The system was heated to 600 °C at 10 °C min^{-1}, held at 600 °C for 6 h, then cooled to 250 °C at 10 °C min^{-1} and kept at this temperature for 12 h, followed by natural cooling to room temperature.

2.2. Preparation of gas diffusion electrodes (GDEs)

For the preparation of the FeP-based GDEs, catalyst inks were developed by mixing 5 mg of the FeP/C catalyst powder, 20 μL Nafion ionomer solution (5% in aliphatic alcohols and water, Sigma Aldrich), 480 μL ethanol, and 500 μL water. The ink suspension was sonicated for 45 min and loaded on C-cloth (GDL-CT, FuelCellsEtc) via air-assisted spray deposition, while the C-cloth substrate was kept constantly at 60 °C for the evaporation of the solvent. The catalyst loading on the GDEs was 0.4 mg FeP cm^{-2}, while Nafion loading was 20%. A commercial Pt/C GDE (0.5 mg Pt cm^{-2}, FuelCellsEtc) was used as a reference material.

2.3. Half-cell electrochemical measurements (Gaskatel cell)

Electrocatalytic activity towards HER and durability of the FeP GDEs was initially evaluated via half-cell measurements (FlexCell HZ-PP01, Gaskatel GmbH) at 22 °C, using 0.5 M H_2SO_4 saturated with nitrogen as electrolyte. Measurements were performed using a three-electrode configuration, where the GDE served as the working electrode and a platinum wire as a counter electrode placed inside the electrolyte chamber. The potentials were measured using a Luggin capillary with a reversible hydrogen electrode (RHE, Hydroflex, Gaskatel GmbH). Linear sweep voltammetry (LSV) was performed with 5 mV s^{-1} towards the cathodic direction, while the *iR* compensation was calculated based on electrochemical impedance spectroscopy using a Vertex potentiostat (Ivium Technologies). LSVs were recorded with both fresh and used electrodes. Used electrodes underwent 1000 consecutive cyclic voltammetry cycles from +50 mV to –300 mV with 50 mV s^{-1} scan rate.

2.4. Fabrication of membrane electrode assemblies and testing in a PEM electrolyzer

For the fabrication of MEAs, the GDEs were attached to commercial half-MEAs of Nafion 115/$IrRuO_x$ (3 mg cm^{-2}) purchased from FuelCellsEtc. The MEAs were introduced in an

in-house built PEM electrolysis cell with 5 cm^2 active area. A Pt–Ti mesh was used for the anode's current collection. Water was circulated in both anodic and cathodic chambers at a rate of 10 mL h^{-1} using a peristaltic pump (Masterflex C/L). The PEM water electrolyzer was constantly kept at 22 °C and its performance was evaluated using a Vertex potentiostat (Ivium Technologies). The polarization data were recorded by applying constant potentials between 1.2 V and 2.2 V, with a stabilization time of 10 min at each step.

2.5. PEM water electrolysis coupled to product analysis by mass spectrometer

To enable product analysis, water was supplied to the anodic compartment of the PEM electrolyzer with a peristaltic pump (Masterflex, C/L) at 10 mL h^{-1}, while the cathodic compartment was supplied with ultrapure He (99.999%) passing through a thermostated H_2O-containing saturator. The saturator was kept constantly at 40 °C, while all lines were heated at 70 °C to avoid water condensation. The effluent of the cathode was analyzed with a Hiden Analytical HPR20 quadrupole mass spectrometer. A Peltier cell was connected prior to the analysis unit to separate non-condensate water. For the quantification of produced hydrogen, the signal of $m/z = 2$ was used, after calibration with certified hydrogen mixtures.

3. Results and Discussion

The straightforward synthesis of our novel FeP catalyst was carried out by incipient wetness impregnation of iron(III) acetylacetonate precursor, chosen due to its low decomposition temperature of 186 °C,[30] on conductive C support followed by gas transport phosphorization (for details, see Section 2.1.). This approach omits the need of an intermediate iron reduction step to metal. In addition to good conductivity, anchoring on active C offers the advantage of simple impregnation procedure and high surface area as compared to our previously used carbon paper.

According to powder X-ray diffraction analysis, the as-synthesized material is orthorhombic FeP with no evidence of oxides or metallic compounds (Figure S1). An approximate crystallize size of 21 ± 2 nm was calculated from the Scherrer equation. Inductively coupled plasma–optical emission spectrometry revealed an iron content of 20 wt % for the material, and specific surface area of 278 m^2 g^{-1} was determined by N_2 physisorption.

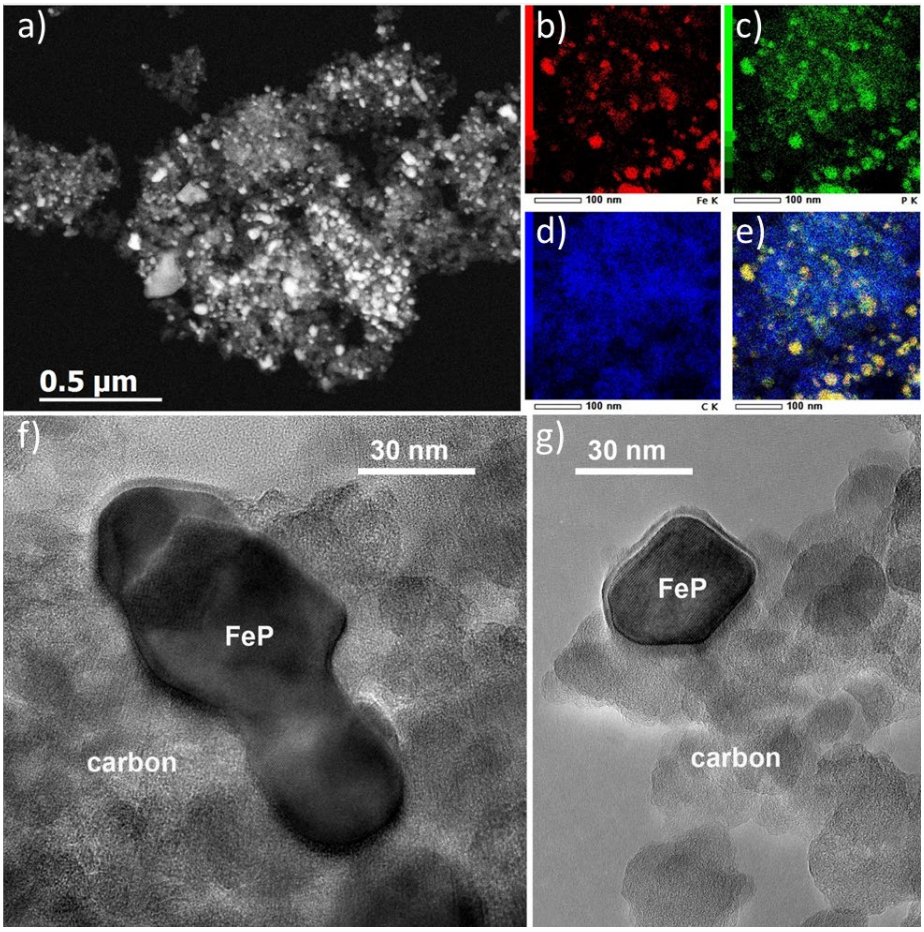

Figure 1. a) HAADF–STEM image of FeP nanoparticles on carbon together with elemental maps for b) Fe, c) P, d) C, and e) their mixture. f, g) Representative TEM images of singular FeP particles anchored on conductive carbon supporting material.

We then examined the composition of the material by high-angle annular dark-field scanning transmission electron microscopy (HAADF–STEM; Figure 1). The FeP nanoparticles show uniform distribution over the carbon support (Figure 1a), as also confirmed by the corresponding energy-dispersive X-ray spectroscopy (STEM–EDX) elemental maps of Fe, P, and C (Figures 1b–e), suggesting that the catalyst is single-phase FeP, devoid of secondary phases. EDX analysis also indicates that the Fe:P ratio is 1:1, which agrees fairly well with the expected sample composition FeP. TEM imaging reveals that the FeP nanoparticles are well-anchored on the C support and exhibit various faceted shapes without signs of agglomeration (Figures 1f–g). The particles are highly crystalline and predominantly expose the [010] facets (Figure 2a,b), as confirmed by selected area electron diffraction. Notably, we recently demonstrated experimentally and theoretically that catalytic activity in HER varies for different crystallographic facets of FeP, with the highest performance shown by the [010] facet.[31] The corresponding STEM–EDX maps of the FeP nanoparticle show the homogeneous distribution of key constituent Fe and P elements without any segregation or presence of C in the structure, indicating phase-purity of the catalyst (Figures 2c–g). The mapping data also suggest the formation of a thin amorphous oxidized layer on the surface of the FeP particles, which is more clearly seen in Figures 2h,i (indicated by arrows). This layer most likely originates from partial surface oxidation, typical for non-oxide nanoparticles.

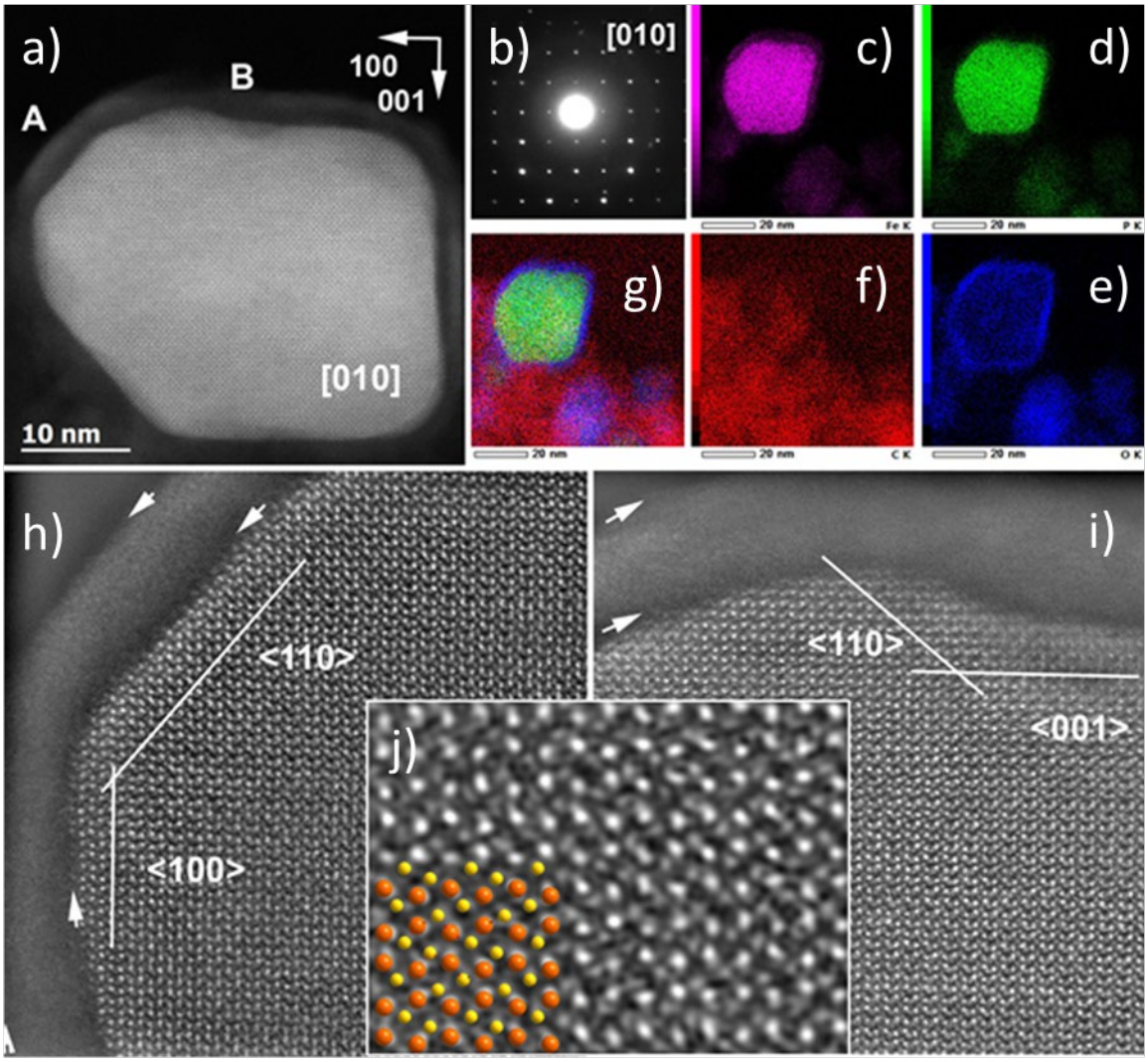

Figure 2. a) Low-magnification and h, i) high-resolution HAADF–STEM images of a FeP nanoparticle along b) [010] zone axis together with the corresponding STEM–EDX element maps for c) Fe, d) P, e) O, f) C, and g) their mixture. j) In the overlaid structural image, Fe is shown as large orange spheres, while P is shown as small yellow spheres.

For the preparation of the gas diffusion electrodes, the FeP/C catalyst was formulated as an ink in ethanol containing Nafion ionomer as binder. After sonication, the ink was deposited onto commercial C-cloth substrates by air-assisted spray deposition at 60 °C. The resulting electrodes

showed FeP loading of 0.4 mg cm^{-2} and 20% dry Nafion loading. Initial investigation of the HER activity and stability of FeP/C gas diffusion electrodes was carried out via half-cell measurements in aqueous acidic 0.5 M H_2SO_4 electrolyte (Figure 3a). The obtained results were compared to those of a commercial Pt/C-cloth electrode (0.5 mg cm^{-2}). To drive cathodic current density of 10 mA cm^{-2}, a potential (η_{10}) of −197 mV was required with FeP/C as compared to −19 mV with Pt. Tafel slopes of $b = 57$ mV dec^{-1} and $b = 29$ mV dec^{-1} were obtained with FeP/C and Pt, respectively (Figure 3b). The performance of our FeP/C electrode compares well with reported TMP-based gas diffusion electrodes at similar catalyst loadings (Table S1). We then probed the stability of our FeP/C electrode by continuous cyclic voltammetry sweeps for 1000 cycles from +50 to −300 mV applied potential *vs* reversible hydrogen electrode (RHE). Figure 3a shows the LSV of the used FeP/C electrode, where only a 20 mV drop was observed compared to the fresh sample, indicating high durability of our electrode. These half-cell measurements served merely as a screening tool, with our ultimate goal being the activity and stability assessment of our FeP catalyst under realistic conditions. Notably, Pt dissolution from the counter electrode could lead to misleading catalytic activity assessment in half-cell measurements.[32] We therefore investigated the performance of the FeP cathodes under full-cell measurements in flow-through conditions using a carefully designed experimental protocol.

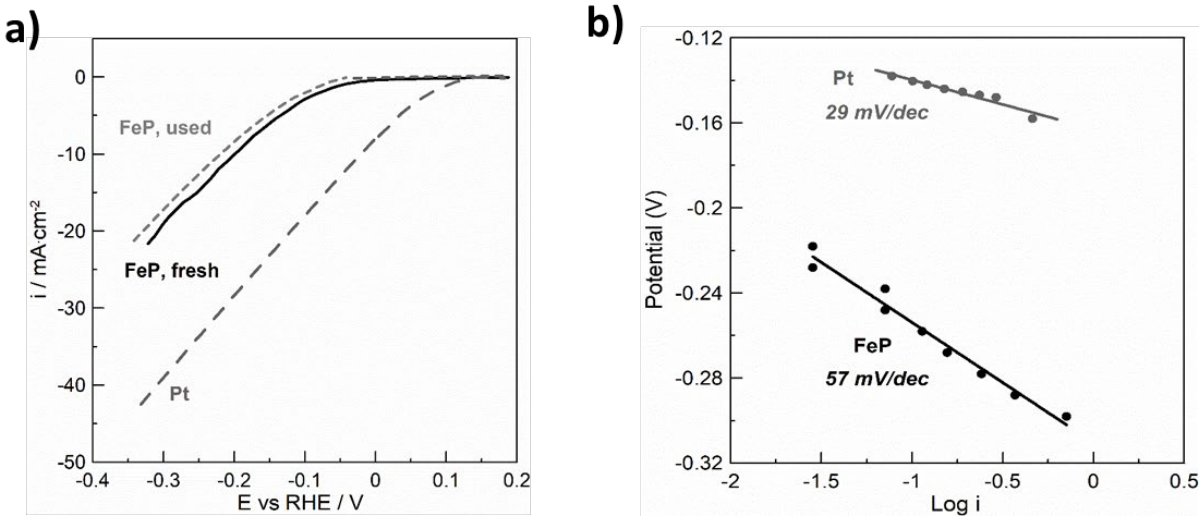

Figure 3. a) Water splitting performance of as-prepared and used (after 1000 CV cycles) FeP on C cloth (mass loading = 0.4 mg cm^{-2}) together with commercial Pt on C-cloth as control (0.5 mg cm^{-2}) toward HER in aqueous 0.5 M H_2SO_4 electrolyte. b) Tafel plots extracted from a), related to the HER performance of FeP- and Pt-based C-cloth electrodes in 0.5 M H_2SO_4.

Although many studies exist on identifying promising electrocatalysts towards HER of earth-abundant elements using half-cell measurements, reports on industrially relevant full-cell PEM water electrolysis are scarce.[6] On the other hand, testing emerging electrocatalysts in full-cell configurations is of great practical importance, since deviations can be expected from half-cell measurements, where mass and ion transfer phenomena are less complex. The few reports on the integration of Pt-free HER electrocatalysts into full-cell PEM water electrolysis devices have mainly dealt with transition metal sulfides.[6,33–40] Implementation of TMPs into MEAs for full-cell testing has so far been realized only for NiP_2[15] and CoP,[41] showing promising results.

To test our FeP-based cathodes in PEM water electrolyzers, MEAs were developed by attaching them to commercial half-cells of Nafion 115 membrane electrolyte and $IrRuO_x$ anode. For comparison, MEAs comprising a state-of-the-art Pt cathode were also measured. The MEAs were operated during water electrolysis at 1 bar and 22 °C and the onset potential is 0.1 V higher for

FeP as compared to the Pt cathode (Figure 4a). A current density of 0.2 A cm^{-2} is achieved at 2.06 V with the FeP cathode *vs* 1.71 V with Pt, corresponding to a difference of only 0.07 W cm^{-2} in power input.

Taking into account typical lifetimes of industrial water electrolyzers of 10,000 h[42] and based on the current electricity prices in the European Union, a country-dependent operational expenditure of 0.04–0.12 € cm^{-2} is required to cover the additional power demands of FeP compared to Pt cathodes. However, this cost is lower than what would be saved in capital expenditure, which accounts for 0.15 € cm^{-2} (for details on cost analysis, see the SI). Since the performance of the FeP cathode can be further improved upon optimization of the electrode features and architecture, the electricity cost has the potential to be further reduced, overall suggesting that FeP holds great promise for practical applications.

When comparing the performance of the few reported PEM water electrolyzers with Pt-free cathodes (Figure 4b), our FeP-based cathode outperforms those tested at similar operating conditions. However, such comparisons are not straightforward since various parameters, such as anode and cathode catalyst loading and Nafion membrane thickness, can affect the overall cell performance. Details on the conditions, catalyst loadings, and performance are provided in Table S2. At 2 V, the highest current densities have been reached at elevated temperatures: 1.1 A cm^{-2} with MoP[34] (3 mg cm^{-2} at 80 °C) and 0.72 A cm^{-2} with both $Ni_{0.64}Co_{0.36}O_xS_{0.28}$[39] and $Cu_{93.7}Mo_{6.3}$[40] (90 °C). At a lower temperature of 50 °C and pressure of 27.6 bar, CoP[43] (1 mg cm^{-2}) gave a current density of 0.88 A cm^{-2}. When comparing results obtained near room temperature, our FeP cathode outperforms the reported catalysts by achieving double the current density to that obtained with NiP_2[15] and MoS_2[35] (0.08 and 0.06 A cm^{-2}, respectively) at 20% of the catalyst loading, highlighting the promising activity of our HER catalyst.

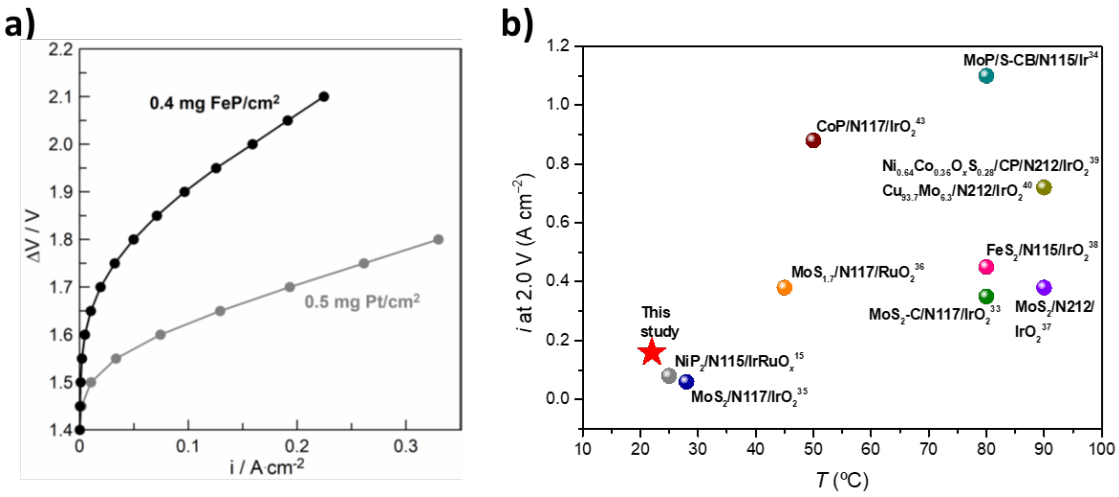

Figure 4. a) Polarization curves during PEM water electrolysis at 22 °C with $IrRuO_x$ anode, Nafion 115, and cathodes based on FeP and Pt. b) Comparison of performance of various PEM water electrolyzers with Pt-free cathodes under 2 V operation. For details of the conditions, see Table S2.

As recently pointed out by Kibsgaard and Chorkendorff,[3] when applying Pt-free electrocatalysts in water electrolyzers, it is of high importance to measure the actual amount of gases produced instead of solely reporting the associated currents. To confirm that the currents we observed correspond to water electrolysis and not to a side reaction, such as change of Fe oxidation state and concomitant phosphine production,[14] we carried out quantitative product analysis on a quadrupole mass spectrometer. To facilitate these experiments, certified ultrapure He was supplied to the cathode side, serving as carrier gas for the produced H_2. Product analysis was carried out by stepping the current from 50 to 300 mA. We found PEM water electrolyzers with the FeP cathode to operate with Faradaic efficiencies between 84% and 100% (Figure 5). At 300 mA, an efficiency of 67.7% was achieved based on the lower heating values of H_2, while the energy consumption of

4.1 kWh Nm^{-3} of produced H_2 was achieved (for the calculation, see the SI), which compares well to reported values with MoS_2 cathode.[44]

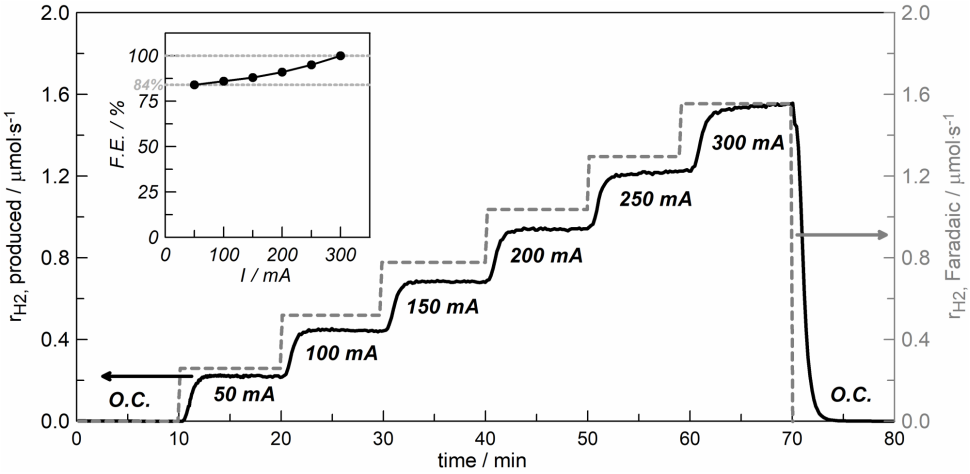

Figure 5. Actual H_2 production rate, based on quantitative product analysis with mass spectrometry (solid black line) and theoretical H_2 production rate, based on Faraday's law (dashed grey line), upon consecutive steps of current application. The inset shows the Faradaic efficiencies as a function of applied current. Data obtained during PEM water electrolysis at 22 °C with $IrRuO_x$ anode, Nafion 115, and FeP cathode.

The durability of Pt-free cathodes under operation in PEM water electrolysis for operating times of >100 h under constant polarization has so far only been demonstrated for MoS_2,[35] FeS_2,[38] and CoP.[43] However, the durability under varying power input remains to be addressed despite its significance to simulate compatibility with intermittent renewable energy sources. Our results show that FeP cathode features excellent stability when tested upon continuous electrolysis under constant polarization at 2 V for 100 h (Figure 6a), and also upon consecutive 4 h steps of shut-down (1.4 V) and switch-on (2.0 V; Figure 6b).

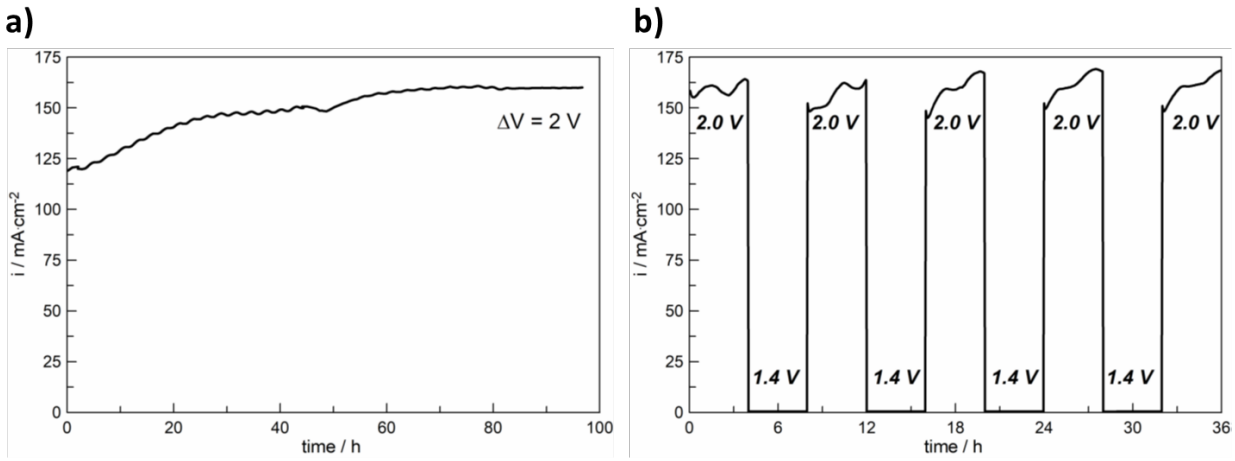

Figure 6. a) Current density during constant polarization at 2 V for 100 h. b) Durability test by consecutive 4 h steps of shut-down (1.4 V) and switch-on (2.0 V). MEA consists of FeP/Nafion 115/$IrRuO_x$ and is operated during PEM water electrolysis at 22 °C.

4. Conclusions

In summary, we have prepared a novel highly crystalline FeP nanocatalyst supported on C through a facile impregnation and phosphorization method. Our crystals feature predominantly exposed [010] facets, accounting for the high activity of the catalyst in hydrogen evolution reaction. We evaluated the FeP cathodes for the first time under application-relevant conditions in a PEM water electrolysis single cell, where our catalyst outperformed other non-precious metal cathodes tested during PEM water electrolysis at similar conditions. Via quantitative product analysis, we provided strong experimental evidence that a PEM water electrolyzer containing the FeP cathode can operate with 84–100% Faradaic efficiencies and with 4.1 kWh Nm^{-3} energy consumption. Finally, excellent durability of our FeP-based electrolyzer was observed upon 100 h operation at 2 V. In relation to coupling PEM water electrolysis to intermittent renewable energy sources, durability of our cell was also investigated upon consecutive switch-on and shut-down cycles for the overall duration of 36 h, showing the suitability of our cathode for renewable energy-driven

H_2 generation. The performance together with our preliminary cost analysis showed the FeP nanocatalyst to have high potential for practical application.

Notes

The authors declare no competing financial interest.

Acknowledgements

We thank CABOT for the samples of conductive carbon. This work was supported by the European Union's Horizon 2020 research and innovation program through the CritCat Project under the Grant Agreement No. 686053. Syngaschem BV acknowledges Mr. Y. Bannink and Mr. K. Buiter for experimental support and Synfuels China Technology (Beijing Huairou, P.R. China) for funding.

Supporting Information

The Supporting Information is available free of charge on the ACS Publications website: Characterization methods, experimental data, cost analysis, and comparison with literature data.

REFERENCES

(1) Pomerantseva, E.; Resini, C.; Kovnir, K.; Kolen'ko, Yu. V. Emerging Nanostructured Electrode Materials for Water Electrolysis and Rechargeable beyond Li-Ion Batteries. *Adv. Phys. X* **2017**, *2*, 211–253.

(2) Callejas, J. F.; Read, C. G.; Roske, C. W.; Lewis, N. S.; Schaak, R. E. Synthesis , Characterization , and Properties of Metal Phosphide Catalysts for the Hydrogen-Evolution Reaction. *Chem. Mater.* **2016**, *28*, 6017−6044.

(3) Kibsgaard, J.; Chorkendorff, I. Considerations for the Scaling-up of Water Splitting Catalysts. *Nat. Energy* **2019**, *4*, 430–433.

(4) Owens-Baird, B.; Kolen'ko, V. Yu.; Kovnir, K. Structure–Activity Relationships for Pt-Free Metal Phosphide Hydrogen Evolution Electrocatalysts. *Chem. Eur. J.* **2018**, *24*, 7298–7311.

(5) Sapountzi, F. M.; Gracia, J. M.; Weststrate, C. J. K.; Fredriksson, H. O. A.; Niemantsverdriet, J. W. Electrocatalysts for the Generation of Hydrogen , Oxygen and Synthesis Gas. *Prog. Energy Combust. Sci.* **2017**, *58*, 1–35.

(6) Sun, X.; Xu, K.; Fleischer, C.; Liu, X.; Grandcolas, M.; Strandbakke, R.; Bjørheim, T. S.; Norby, T.; A, C. Earth-Abundant Electrocatalysts in Proton Exchange Membrane Electrolyzers. *Catalysts* **2018**, *8*, 657.

(7) Serov, A.; Workman, M. J.; Artyushkova, K.; Atanassov, P.; McCool, G.; McKinney, S.; Romero, H.; Halevi, B.; Stephenson, T. Highly Stable Precious Metal-Free Cathode Catalyst for Fuel Cell Application. *J. Power Sources* **2016**, *327*, 557–564.

(8) Workman, M. J.; Dzara, M.; Ngo, C.; Pylypenko, S.; Serov, A.; McKinney, S.; Gordon, J.; Atanassov, P.; Artyushkova, K. Platinum Group Metal-Free Electrocatalysts: Effects of Synthesis on Structure and Performance in Proton-Exchange Membrane Fuel Cell Cathodes. *J. Power Sources* **2017**, *348*, 30–39.

(9) Li, A.; Sun, Y.; Yao, T.; Han, H. Earth-Abundant Transition-Metal-Based Electrocatalysts for Water Electrolysis to Produce Renewable Hydrogen. *Chem. Eur. J.* **2018**, *24*, 18334–18355.

(10) Li, Y.; Dong, Z.; Jiao, L. Multifunctional Transition Metal-Based Phosphides in Energy-Related Electrocatalysis. *Adv. Energy Mater.* https://doi.org/10.1002/aenm.201902104.

(11) Wang, X.; Kolen'ko, Yu. V.; Bao, X.-Q.; Kovnir, K.; Liu, L. One-Step Synthesis of Self-Supported Nickel Phosphide Nanosheet Array Cathodes for Efficient Electrocatalytic Hydrogen Generation. *Angew. Chem. Int. Ed.* **2015**, *54*, 8188–8192.

(12) Lado, J. L.; Wang, X.; Paz, E.; Carbó-Argibay, E.; Guldris, N.; Rodríguez-Abreu, C.; Liu, L.; Kovnir, K.; Kolen´ko, Yu. V. Design and Synthesis of Highly Active Al−Ni−P Foam Electrode for Hydrogen Evolution Reaction. *ACS Catal.* **2015**, *5*, 6503−6508.

(13) Wang, X.; Kolen'ko, Yu. V.; Liu, L. Direct Solvothermal Phosphorization of Nickel Foam to Fabricate Integrated Ni_2P-nanorods/Ni Electrodes for Efficient Electrocatalytic Hydrogen Evolution. *Chem. Commun.* **2015**, *51*, 6738–6741.

(14) Costa, J. D.; Lado, J. L.; Carbó-Argibay, E.; Paz, E.; Gallo, J.; Rodríguez-Abreu, C.; Kovnir, K.; Kolen'ko, Yu. V. Electrocatalytic Performance and Stability of Nanostructured Fe−Ni Pyrite-Type Diphosphide Catalyst Supported on Carbon Paper. *J. Phys. Chem. C* **2016**, *120*, 16537−16544.

(15) Owens-Baird, B.; Xu, J.; Petrovykh, D. Y.; Bondarchuk, O.; Ziouani, Y.; Gonza, N.; Yox, P.; Sapountzi, F. M.; Niemantsverdriet, H.; Kolen'ko, Yu. V; Kovnir, K. NiP_2: A Story of Two Divergent Polymorphic Multifunctional Materials. *Chem. Mater.* **2019**, *31*, 3407−3418.

(16) Xu, Y.; Wu, R.; Zhang, J.; Shi, Y.; Zhang, B. Anion-Exchange Synthesis of Nanoporous FeP Nanosheets as Electrocatalysts for Hydrogen Evolution Reaction. *Chem. Commun.* **2013**, *49*, 6656–6658.

(17) Zhang, Z.; Lu, B.; Hao, J.; Yang, W.; Tang, J. FeP Nanoparticles Grown on Graphene Sheets as Highly Active Non-Precious-Metal Electrocatalysts for Hydrogen Evolution Reaction. *Chem. Commun.* **2014**, *50*, 11554–11557.

(18) Liu, R.; Gu, S.; Du, H.; Li, C. M. Controlled Synthesis of FeP Nanorod Arrays as Highly Efficient Hydrogen Evolution Cathode. *J. Mater. Chem. A* **2014**, *2*, 17263–17267.

(19) Jiang, P.; Liu, Q.; Liang, Y.; Tian, J.; Asiri, A. M.; Sun, X. A Cost-Effective 3D Hydrogen Evolution Cathode with High Catalytic Activity: FeP Nanowire Array as the Active Phase. *Angew. Chem. Int. Ed.* **2014**, No. 21175129, 12855–12859.

(20) Zhang, Z.; Hao, J.; Yang, W.; Lu, B.; Tang, J. Modifying Candle Soot with FeP Nanoparticles into High-Performance and Cost-Effective Catalysts for the Electrocatalytic Hydrogen Evolution Reaction. *Nanoscale* **2015**, *7*, 4400–4405.

(21) Yan, Y.; Thia, L.; Xia, B. Y.; Ge, X.; Liu, Z.; Fisher, A.; Wang, X. Construction of Efficient 3D Gas Evolution Electrocatalyst for Hydrogen Evolution: Porous FeP Nanowire Arrays

on Graphene Sheets. *Adv. Sci.* **2015**, *2*, 1500120.

(22) Han, S.; Feng, Y.; Zhang, F.; Yang, C.; Yao, Z.; Zhao, W.; Qiu, F.; Yang, L.; Yao, Y.; Zhuang, X.; Feng, X. Metal-Phosphide-Containing Porous Carbons Derived from an Ionic-Polymer Framework and Applied as Highly Efficient Electrochemical Catalysts for Water Splitting. *Adv. Funct. Mater.* **2015**, *25*, 3899–3906.

(23) Son, C. Y.; Kwak, I. H.; Lim, Y. R.; Park, J. FeP and FeP_2 Nanowires for Efficient Electrocatalytic Hydrogen Evolution Reaction. *Chem. Commun.* **2016**, *52*, 2819–2822.

(24) Zhu, X.; Liu, M.; Liu, Y.; Chen, R.; Nie, Z.; Li, J.; Yao, S. Carbon-Coated Hollow Mesoporous FeP Microcubes: An Efficient and Stable Electrocatalyst for Hydrogen Evolution. *J. Mater. Chem. A* **2016**, *4*, 8974–8977.

(25) Lv, C.; Peng, Z.; Zhao, Y.; Huang, Z.; Zhang, C. The Hierarchical Nanowires Array of Iron Phosphide Integrated on a Carbon Fiber Paper as an Effective Electrocatalyst for Hydrogen Generation. *J. Mater. Chem. A* **2016**, *2*, 1454–1460.

(26) Li, D.; Liao, Q.; Ren, B.; Jin, Q.; Cui, H.; Wang, C. A 3D-Composite Structure of FeP Nanorods Supported by Vertically Aligned Graphene for the. *J. Mater. Chem. A* **2017**, *5*, 11301–11308.

(27) Du, Y.; Li, Z.; Liu, Y.; Yang, Y.; Wang, L. Nickel-Iron Phosphides Nanorods Derived from Bimetallic-Organic Frameworks for Hydrogen Evolution Reaction. *Appl. Surf. Sci.* **2018**, *457*, 1081–1086.

(28) Shi, S. Y.; Zhang, B. Recent Advances in Transition Metal Phosphide Nanomaterials: Synthesis and Applications in Hydrogen Evolution Reaction. *Chem. Soc. Rev.* **2016**, *45*, 1529.

(29) Yu, Y.; Ma, J.; Chen, C.; Fu, Y.; Wang, Y.; Li, K.; Liao, Y.; Zheng, L.; Zuo, X. General Method for Synthesis Transition-Metal Phosphide / Nitrogen and Phosphide Doped Carbon Materials with Yolk-Shell Structure for Oxygen Reduction Reaction. *ChemCatChem* **2019**, *11*, 1722–1731.

(30) Song, Q.; Ding, Y.; Wang, Z. L.; Zhang, Z. J. Tuning the Thermal Stability of Molecular Precursors for the Nonhydrolytic Synthesis of Magnetic $MnFe_2O_4$ Spinel Nanocrystals. *Chem. Mater.* **2007**, *19*, 4633–4638.

(31) Owens-Baird, B.; Sousa, J. P. S.; Ziouani, Y.; Petrovykh, D.; Zarkevich, N. A.; Johnson, D. D.; Kolen'ko, Yu. V.; Kovnir, K. Crystallographic Facet Selective HER Catalysis: Exemplified in FeP and NiP_2 Single Crystals. *Submitted*.

(32) Chen, R.; Yang, C.; Cai, W.; Wang, H.-Y.; Miao, J.; Zhang, L.; Chen, S.; Liu, B. Use of Platinum as the Counter Electrode to Study the Activity of Nonprecious Metal. *ACS Energy Lett.* **2017**, *2*, 1070−1075.

(33) Corrales-Sánchez, T.; Ampurdanés, J.; Urakawa, A. MoS_2-Based Materials as Alternative Cathode Catalyst for PEM Electrolysis. *Int. J. Hydrogen Energy* **2014**, *9*, 20837–20843.

(34) Ng, J. W. D.; Hellstern, T. R.; Kibsgaard, J.; Hinckley, A. C.; Benck, J. D.; Jaramillo, T. F. Polymer Electrolyte Membrane Electrolyzers Utilizing Non-Precious Mo-Based Hydrogen Evolution Catalysts. *ChemSusChem* **2015**, *8*, 3512–3519.

(35) Kumar, S. M. S.; Selvakumar, K.; Thangamuthu, R.; Selvi, A. K.; Ravichandran, S.; Sozhan, G.; Rajasekar, K.; Navascues, N.; Irusta, S. Hydrothermal Assisted Morphology Designed MoS_2 Material as Alternative Cathode Catalyst for PEM Electrolyser Application. *Int. J. Hydrogen Energy* **2016**, *41*, 13331–13340.

(36) Lu, A.-Y.; Yang, X.; Tseng, C.-C.; Min, S.; Lin, S.-H.; Hsu, C.-L.; Li, H.; Idriss, H.; Kuo, J.-L.; Huang, K.-W.; et al. High-Sulfur-Vacancy Amorphous Molybdenum Sulfide as a High Current Electrocatalyst in Hydrogen Evolution. *Small* **2016**, *12*, 5530–5537.

(37) Kim, J. H.; Kim, H.; Kim, J.; Lee, H. J.; Jang, J. H.; Ahn, S. H. Electrodeposited Molybdenum Sulfide as a Cathode for Proton Exchange Membrane Water Electrolyzer. *J. Power Sources* **2018**, *392*, 69–78.

(38) Giovanni, C. Di; Reyes-Carmona, Á.; Coursier, A.; Nowak, S.; Grenèche, J.-M.; Lecoq, H.; Mouton, L.; Rozière, J.; Jones, D.; Peron, J.; Giraud, M.; Tard, C. Low-Cost Nanostructured Iron Sulfide Electrocatalysts for PEM Water Electrolysis. *ACS Catal.* **2016**, *6*, 2626–2631.

(39) Kim, H.; Kim, J.; Kim, S.-K.; Ahn, S. H. A Transition Metal Oxysulfide Cathode for the Proton Exchange Membrane Water Electrolyzer. *Appl. Catal. B Environ.* **2018**, *232*, 93–100.

(40) Kim, H.; Hwang, E.; Park, H.; Lee, B.-S.; Jang, J. H.; Kim, H.-J.; Ahn, S. H.; Kim, S.-K. Non-Precious Metal Electrocatalysts for Hydrogen Production in Proton Exchange Membrane Water Electrolyzer. *Appl. Catal. B Environ.* **2017**, *206*, 608–616.

(41) Yang, X.; Lu, A.; Zhu, Y.; Hedhili, M. N.; Min, S.; Huang, K.-W.; Han, Y.; Li, L. CoP Nanosheet Assembly Grown on Carbon Cloth: A Highly Efficient Electrocatalyst for Hydrogen Generation. *Nano Energy* **2015**, *15*, 634–641.

(42) Schmidt, O.; Gambhir, A.; Staffell, I.; Hawkes, A.; Nelson, J.; Few, S. Future Cost and Performance of Water Electrolysis: An Expert Elicitation Study. *Int. J. Hydrogen Energy* **2017**, *42*, 30470–30492.

(43) King, L. A.; Hubert, M. A.; Capuano, C.; Manco, J.; Danilovic, N.; Valle, E.; Hellstern, T. R.; Ayers, K.; Jaramillo, T. F. A Non-Precious Metal Hydrogen Catalyst in a Commercial Polymer Electrolyte Membrane Electrolyser. *Nat. Nanotechnol.* **2019**, *14*, 1071–1074.

(44) Sarno, M.; Ponticorvo, E. High Hydrogen Production Rate on RuS_2@MoS_2 Hybrid Nanocatalyst by PEM Electrolysis. *Int. J. Hydrogen Energy* **2018**, *4*, 4398–4405.